

## Vibration Reduction via Constrain Layer Damping Techniques

Mr. John F. Schultze and Dr. John B. Kosmatka

Department of Mechanical Engineering  
Virginia Polytechnic Institute and State University  
Blacksburg, Virginia

### ***Abstract***

Experimental methods to extract loss factors in constrain layer damped beams are compared. Comparison of integral and additive damping treatments are considered. Investigation of partial coverage treatment relation between application length and effective damping ratio for isotropic beams is performed. Results indicate that optimum length exist for cantilever first mode, while the other modes of investigation, clamped/clamped first and second and cantilever second, show consistent increase in effective damping with increase in application length. Integrally damped composite beams show significant increase in damping ratio without reduction in bending stiffness. Log decrement appears to be the best method for measuring damping values for cantilever first mode. Real and Imaginary components extract data that agree well with each other, while forming an upper bound for the log decrement method.

## ***Introduction***

Structural vibration is a recurring problem in such diverse fields from machinery silencing in mining equipment to response attenuation in composite aerospace structures. In current aerospace design, use of composite materials allows the engineer to tailor a material to meet application requirements of mass and stiffness. Vibrations, which cause cyclic loading of a structure, considerably reduce fatigue life thereby increasing failure rate. The use of viscoelastic materials to attenuate response of structures through increasing the composite damping has gained popularity in recent years. Discussions on the use of viscoelastics are presented by Mar <sup>1</sup>.

The evaluation of one damping technique is often done through experimentation. A comparison of several techniques will be presented. Evaluation of partial coverage and integrally damped structures will also be pursued.

Passive damping seems the most effective technique for structures that have limited number of modes of concern. One major technique is Constrain Layer Damping (CLD). This method involves sandwiching a viscoelastic medium between two stiff outer layers. The viscoelastic, a rubber-like compound, dissipates energy via shear deformation. The two outer layers undergo the significant bending and extensional loads while the central withstands the shear forces. The incorporation of viscoelastic materials into existing structures (via CLD) has been thoroughly investigated by numerous researchers<sup>2-15</sup>.

Viscoelastic damping is incorporated in one of two ways; 1.) additive damping tape or 2.) integrally incorporated damping central layer. The additive damping tapes have been used in an ad-hoc method to solve existing vibration problems. Partial coverage with damping tapes allows the treatment to be applied in the area and amount to effect the desired result for some applications. Integrally damped structures are a relatively new phenomena. The damping layer is often sandwiched between two symmetric constraining layers. Two sets of boundary conditions, cantilever and clamped/clamped, are investigated for the partial coverage treatment on an isotropic beam. The integrally damped beams are subjected to cantilever investigation only.

The rationale behind investigating partial coverage treatments is twofold; first, determine level of damping treatment will meet design criteria, and second, investigate possibility of an optimum length of treatment for a given mode and structure. The driving force behind investigation of integrally damped beams is; to determine effect of damping incorporated within design of beam and located in center of symmetric beam. It is obvious that integrally damped beams involve additional steps in manufacture and design. In the beams investigated here, the two additional steps of; 1.) special lay-up with pre-cured graphite/epoxy composite and 2.) pressure bonding of the damping material to the composite, were required. Another design consideration in the incorporation of additive damping is weight, compared with graphite epoxy the density is about equal, with the damping tape on isotropic aluminum beam the density is also about the same (the backing is the significant factor). Experimental method comparisons are neces-

sary because it is not always feasible to run the best suited test. Citing this, it must be known how test results correlate with actual values.

The principle objectives of this paper are to investigate different experimental methods to extract damping values for beams with simple boundary conditions and to evaluate partial coverage and integrally damped beams. This survey will be useful to designers and analysts of advanced aerospace structures where fatigue is a significant problem. The two boundary conditions considered are a fixed/fixed (spar-like) beam and a cantilever member (similar to wings and other rotary wing structures) (refer Figure 1.a,b). The research is conducted using experimental results which can later be compared with analytical and finite element models.

## ***Experimental Methods and Formulations***

The two basic frameworks that most structural dynamics experimentation are performed in are; 1.) time domain and 2.) frequency domain. Frequency domain techniques such as a Fast Fourier Transform (FFT) to develop a Frequency Response Function (FRF) are often used. This function, FRF, then is used to extract modal information of natural frequency, modes shapes, damping and other frequency dependent structural properties. This technique assumes linear damping. The primary technique in the time domain is the Log Decrement Time History (LDTH). This model does not assume linear damping but can not give mode shape information readily.

### **Frequency Response Methods**

Three basic FRF methods used in this investigation are; 1.) Real component of the FRF ( $\text{Re}(\text{FRF})$ ), 2.) Imaginary component of the FRF ( $\text{Im}(\text{FRF})$ ), and 3.) Circle Fit of Nyquist plot data. Looking at the imaginary part of the accelerance FRF (ref Figure 2.a), for a single degree of freedom system (SDOF),

$$\text{Im}(\text{FRF}) = \frac{2\zeta \frac{\omega_n}{\omega}}{\left(1 - \left(\frac{\omega_n}{\omega}\right)^2\right)^2 + \left(2\zeta \frac{\omega_n}{\omega}\right)^2} \quad (1.)$$

where  $\omega_n = \sqrt{\frac{k}{m}}$ ,  $\omega$  is the driving frequency and  $\zeta$  is the damping ratio. It can be shown that the maximum response, or resonance, is near the natural frequency (within 1-3 %) for moderate damping ( $\zeta < .05$ ), and has a magnitude of,

$$\text{Im}(\text{FRF})_r \cong \frac{1}{2\zeta} = m \frac{\ddot{X}}{F} \quad (2.)$$

where  $\ddot{X}$ ,  $F$ , and  $m$  are the acceleration, magnitude of the driving force and effective mass. By looking at a point, b, near resonance a relation for relative magnitudes can be developed;

$$Im(FRF)_b = \frac{2\zeta \frac{\omega_n}{\omega_b}}{\left(1 - \left(\frac{\omega_n}{\omega_b}\right)^2\right)^2 + \left(2\zeta \frac{\omega_n}{\omega_b}\right)^2} \cong \frac{\ddot{X}_b}{\ddot{X}_r} \frac{1}{2\zeta}. \quad (3.)$$

Let

$$\frac{\omega_n}{\omega_b} = D ; \quad \frac{\ddot{X}_b}{\ddot{X}_r} = R. \quad (4.a,b)$$

By incorporating equations 4.a and 4.b into equation 3. and restructuring the result, it can be seen;

$$\zeta \cong \frac{|1 - D^2|}{2\sqrt{D\left(\frac{1}{R} - D\right)}}. \quad (5.)$$

Looking at the real part of the accelerance FRF (ref Figure 2.b), SDOF,

$$Re(FRF) = \frac{1 - \left(\frac{\omega_n}{\omega}\right)^2}{\left(1 - \left(\frac{\omega_n}{\omega}\right)^2\right)^2 + \left(2\zeta \frac{\omega_n}{\omega}\right)^2}, \quad (6.)$$

where  $\omega_n$ ,  $\omega$  and  $\zeta$  are defined as before. The point at which this function crosses the zero axis is the natural frequency  $\omega_n$ . It can also be shown that

$$\left(\frac{\omega_n}{\omega_{\min}}\right)^2 = 1 \pm 2\zeta, \quad \left(\frac{\omega_n}{\omega_{\max}}\right)^2 = 1 \pm 2\zeta, \quad (7.a,b)$$

where  $\omega_{\min}$  and  $\omega_{\max}$  are the frequencies of maximum and minimum values of response. While one will occur one each side of the crossing frequency, which will have a higher frequency is dependent of the mode shape of response. From this it is obvious that;

$$\zeta = \frac{1 \mp \left(\frac{\omega_n}{\omega_{\max}}\right)^2}{2}, \quad \frac{1 \mp \left(\frac{\omega_n}{\omega_{\min}}\right)^2}{2}. \quad (8.a,b)$$

Circle fit theory is of a much more complicated nature and can be referenced in Ewins<sup>16</sup> and Luk and Mitchell<sup>17</sup>. Basically it involves constructing a plot of the real versus imaginary components of the FRF into a Nyquist plot. It can then be shown that the developed circle has a diameter inversely proportional to the damping constant,  $\zeta$ . This plot is only truly a circle for the mobility FRF for viscous damping and the dynamic compliance FRF for structural damping. In the case of light damping, less than 1 percent most models work well. Two other frequently used methods are the magnitude of the total FRF and the phase angle of the FRF (refer Figure 3.a.,b).

## Log Decrement Method

The log decrement method entails exciting a structure and measuring the decay of the cyclic vibration when the exciter is removed. From the relative amplitude of successive cycles of vibration and period of damped vibration,  $\tau_d$ , the damped natural frequency,  $\omega_d$ , damping ratio, and natural frequency,  $\omega_n$ , can be extracted. The log of relative amplitudes of successive cycles is called the log decrement,  $\delta$  and is defined as;

$$\delta = \ln \frac{x_i}{x_{i+1}} = \frac{1}{n} \ln \frac{x_i}{x_{i+n}} \quad (9.)$$

where,  $x_i$ ,  $x_{i+1}$ , and  $x_{i+n}$  are amplitude of response at those points in time. From this, for light damping ( $\zeta < .03$ ), it can be shown;

$$\zeta = \frac{\delta}{2\pi} \quad , \quad \omega_d = \frac{2\pi}{\tau_d} \quad (10.a,b)$$

Through plotting, log decrement results, on semi-log paper one can determine easily (often visually) if the damping is indeed linear or of another relation.

## Experimental Results

Looking first at the results of the partial coverage experimentation, (refer Figure 4.a,b and 5.a,b), the structure tested here was a isotropic beam of Aluminum 6061-T6 with damping treatment of ISD-112 (from 3M), a viscoelastic material. The physical dimensions were; for the base beam 9.00 (l) by .875 (w) by .125 (t), the damping treatment was .875 (w) by .005 (t) for the viscoelastic and .010 (t) for the aluminum backing material (all dimensions inches). The application length, A, of the treatment was varied in 25 percent increments of total length, L, (A/L = 0,25,50,75,100%).

The cantilever first mode shows good agreement between real and imaginary FRF techniques. The log decrement graph reports lower damping values and an earlier peak than the FRF methods. The circle fit data, though in a loosely related pattern, doesn't provide useful information about this mode. It appears that the FRF methods bound the log decrement methods from above. Both show a peak in the neighborhood of 50 % (A/L). This is in agreement with previous authors work. The circle fit data discrepancy is due in part to the moderate damping values, decision to use viscous damping model, and the use of accelerance FRF.

The cantilever second mode shows good agreement between real, imaginary, and circle fit methods up to 75 % (A/L). This graph also shows that there is a continual gain in damping with increasing application length.

The fixed/fixed first mode shows less than ten percent deviation for the entire test between all methods used. It also shows that the damping ratio increases consistently with increasing treatment in an almost linear fashion.

The fixed/fixed second mode shows significant deviation in the methods. This difference reaches a maximum of 40 % at an application length of 50 % between the Re(FRF) and circle fit methods. The complement of the test has more reasonable 20 % or less deviations. The main cause in this error is attributable to the low resolution of this high frequency mode.

The time domain approach, as previously mentioned, compared well with the frequency response methods for the cantilever first mode. For the integrally damped beams the effects are not as readily apparent. The first beam was a 3-ply graphite-epoxy laminate [90/0/90] (refer Figure 6.a). This beam was used as a building block for the successive beams. By extracting the damping of this structure, future beams could be thought of as three layer beams with this as one of the layers. The second beam was constructed of two of these laminates surrounding a 10 mil layer of polypropylene (refer Figure 6.b). This increased the bending moment of inertia thereby increasing the relative bending stiffness. The next beam replaced the polypropylene with damping material (ISD-112 from 3M) of equal thickness (refer Figure 7.a). This was designed to increase damping while not effecting stiffness significantly. The final beam was constructed two of the laminates, similar to the third beam, subsisted of sandwiching a 10 mil thick layer of polypropylene (refer Figure 7.b).

The first beam had a damping constant of 1.2%. The second beam reported a value of .4% damping, this is in part due to the increased moment and the slight stiffening the polypropylene gives the beam. The third beam reports a value of 11% damping, demonstrating the significant effect integral damping can achieve. Note also that the natural frequency did not change greatly, indicating that the bending stiffness was not adversely effected. The last beam reports the same value for damping as the third. The natural frequency of the fourth beam is much less than the third which may show that the central layers are not adding much stiffness mainly weight. The plot of integrally damped beam response on semi-log format shows a nearly linear relation, indicating close to linear damping, (refer Figures 8.a.,b).

## ***Conclusions***

The partial treatment shows an optimum for the first mode cantilever in there neighborhood of 50 % (A/L) application length. The second modes of clamped/clamped and cantilever in addition to first mode clamped/clamped show consistently increasing damping with increasing application length.

The incorporation of damping material in the central part of the structure appears to be the most efficient method to increase damping.

The frequency domain techniques of the Real and Imaginary components of the FRF agree reasonably well with each other for the light damping investigated here, but care must be taken to assure sufficient spectral resolution of test. They also appear to be an upper bound for the log decrement method. The circle fit data must be re-evaluated using a mobility FRF model.

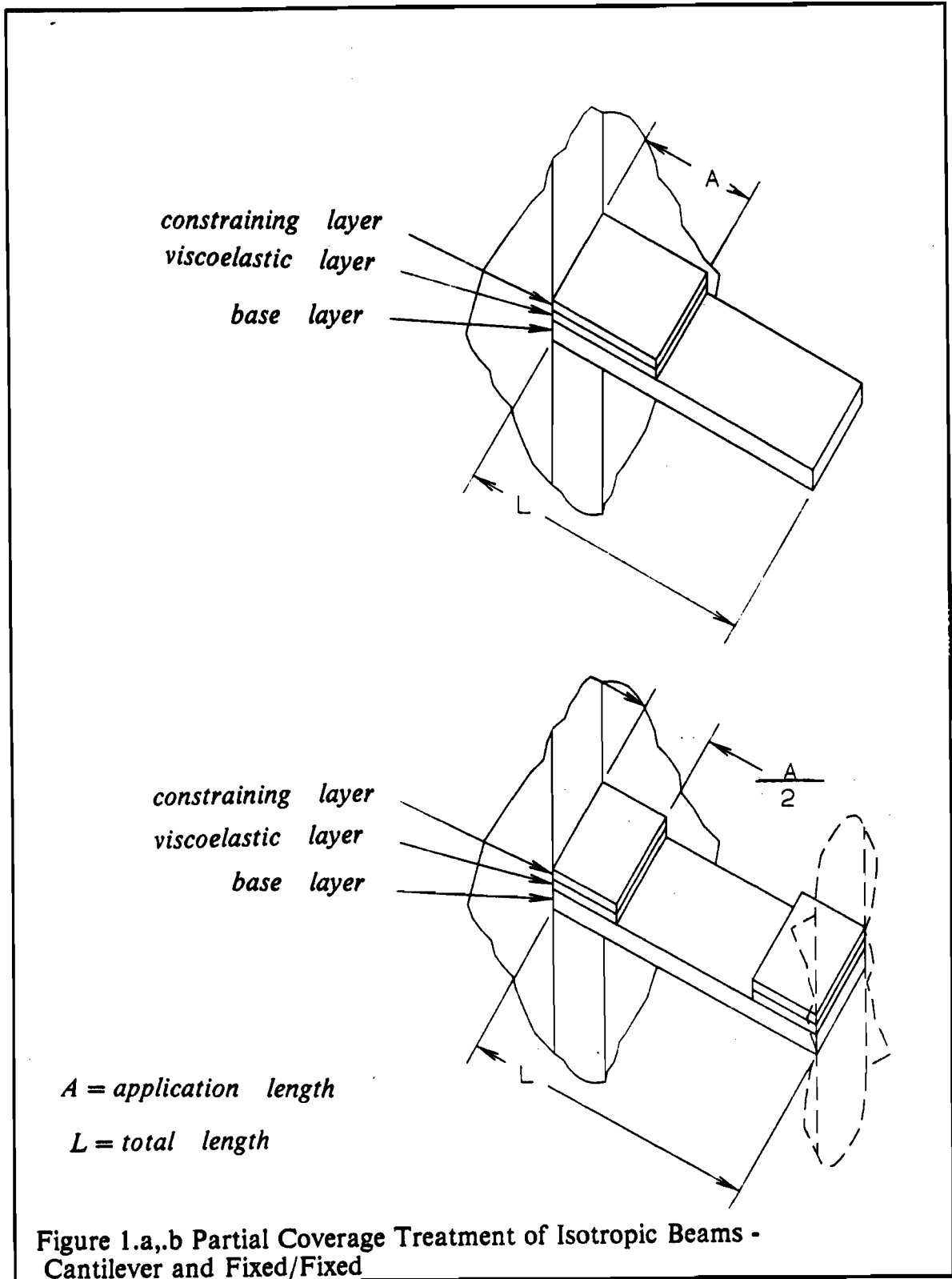
The log decrement tests show that damping is fairly linear for all the beams tested. Also the test showed peaks in the expected region for the case of cantilever first mode.

## **REFERENCES**

1. Mar, J. W. ; "Some Musings on How to Make Damping a Creative Force in Design" *Vibration Damping 1984 Workshop Proceedings*, Wright-Patterson Air Force Base, November, 1984.
2. Oberst, H. "ueber die Dämpfung der Biegeschwingungen dünner Bleche durrch fest haftende Belage," *Acustica*, Vol.2, Akustische Beihefte No.4, 1952, pp.181-194. (Translation by H.L. Blackford, Inc., 24 Commerce St., Newark, N.J.)
3. Ross, D., Ungar, E.E., and Kerwin, Jr., E.M., "Damping of Flexural Vibrations by Means of Viscoelastic Laminae," Section III *Structural Damping*, ASME, New York, NY, 1959.
4. DiTaranto, R. A.; "Effect of End Constraints on the Damping of Laminated Beams" *The Journal of the Acoustical Society of America*, Vol. 39, No. 2, 1966, pp. 405-407.
5. DiTaranto, R. A. and W. Blasingame; "Effect of End Constraints on the Damping of Laminated Beams" *The Journal of the Acoustical Society of America*, Vol. 39, No. 2, 1966, pp. 405-407.
6. DiTaranto, R. A. and W. Blasingame; "Composite Damping of Sandwich Beams" *Journal of Engineering for Industry*, November, 1967, pp. 633-638.
7. Mead, D.J., and Markus, S., "The Forced Vibration of Three-Layer, Damped Sandwich Beams with Arbitrary Boundary Conditions," *Journal of Sound and Vibration*, Vol. 10, No. 2, 1969, pp. 163-175.
8. Mead, D.J., and Markus, S., "Loss Factors and Resonant Frequencies of Encastre' Damped Sandwich Beams," *Journal of Sound and Vibration*, Vol. 12, No. 1, 1970, pp. 99-112.

9. Mead, D.J., "Governing Equations for Vibrating Constrained-Layer Damping Plates and Beams," *Journal of Applied Mechanics*, June, 1973, pp. 639-640.
10. Kerwin, E. M. Jr., "Damping of Flexural Waves by a Constrained Viscoelastic Layer," *The Journal of the Acoustical Society of America*, Vol. 31, No. 7, 1959, pp. 952-962.
11. Rao, D. K., "Frequency and Loss Factors of Sandwich Beams Under Various Boundary Conditions," *Journal of Mechanical Engineering Science*, Vol. 20, No. 5, 1978, pp. 271-282.
12. Drake, M. L., "A different Approach to 'Designed In' Passive Damping" *Shock and Vibration Bulletin* No. 55, June, 1985, pp. 109-117
13. Carne, T.; "Constrained Layer Damping Examined By Finite Element Analysis"; Society of Engineering Science 12th Annual Meeting, Austin, Texas, 20-22 October 1975, Proceedings of the University of Texas, 1975, pp. 567-576.
14. Liguore, S. L.; "Evaluation of Analytical Methods to Predict Constrained-Layer Damping Behavior" Virginia Polytechnic Institute and State University, **Master's Thesis**, May, 1988.
15. Liguore, S. L. and J. B. Kosmatka ; "Evaluation of Analytical Methods to Predict Constrained-Layer Damping Behavior" Proceedings of the Sixth International Modal Conference, February, 1988. pp 421-427.
16. Ewins, D. J. *Modal Testing: Theory and Practice* Research Studies Press LTD, Letchworth Hertfordshire, England, 1986. pp 153-170.
17. Luk, Y. W. and L. D. Mitchell; "System Identification of Via Modal Analysis" *Modal Testing and Refinement*, AMD-59, Ed: D. F. H. Chu, ASME, Nov. 13-18, 1983, pp. 31-49.





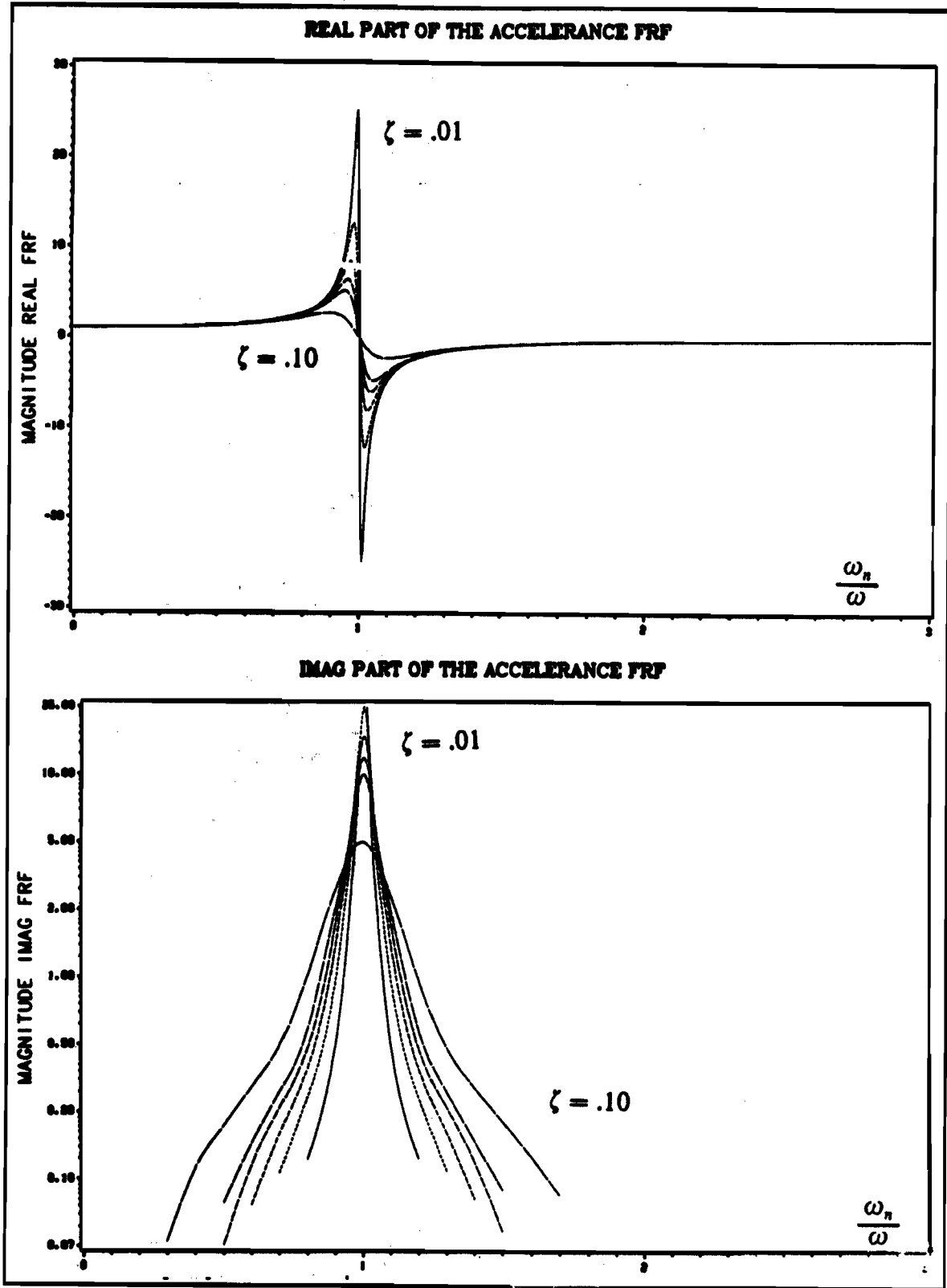


Figure 2.a,.b Imaginary and Real Components of FRF -  $\zeta$  from .01 to .10

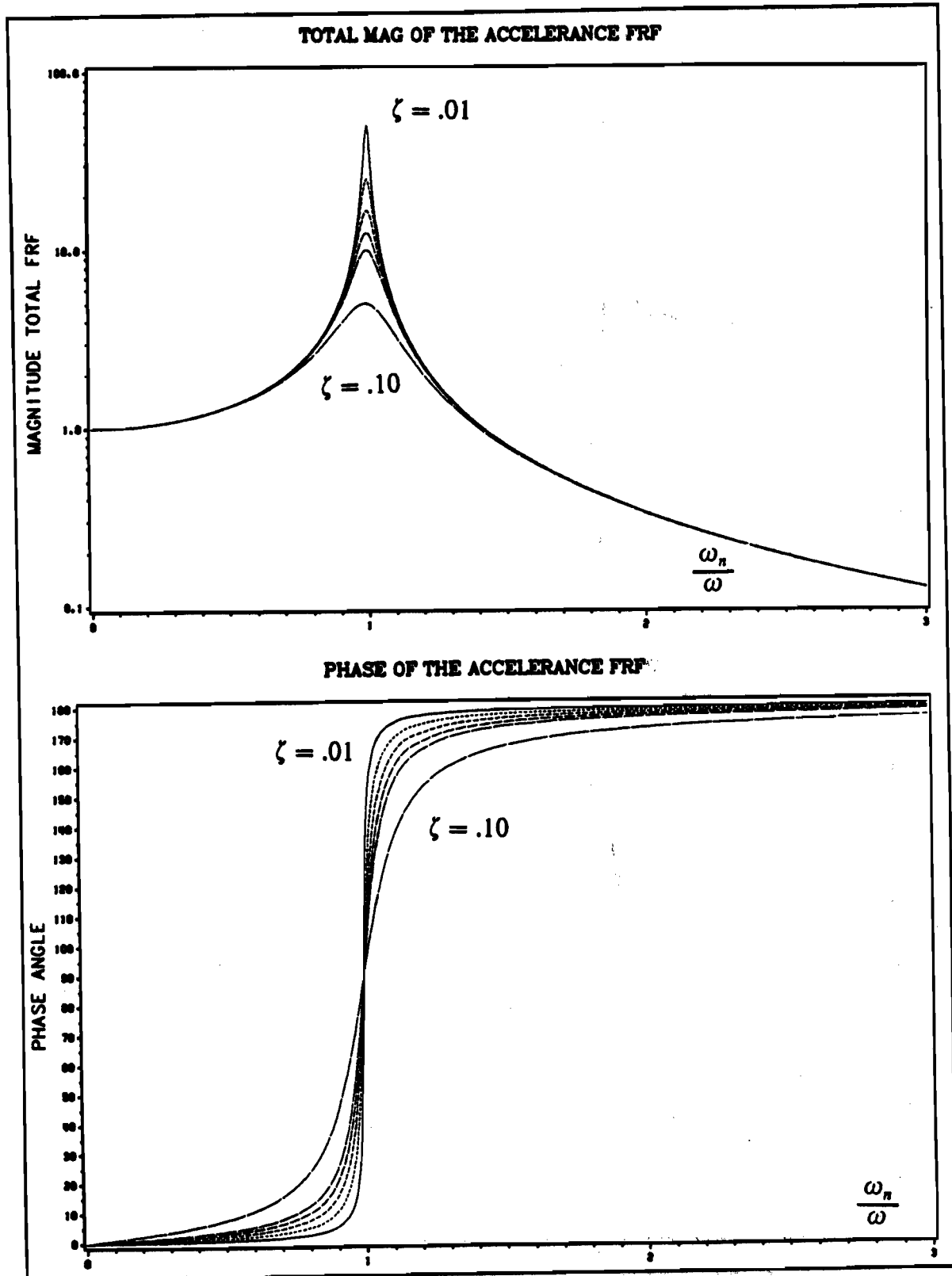
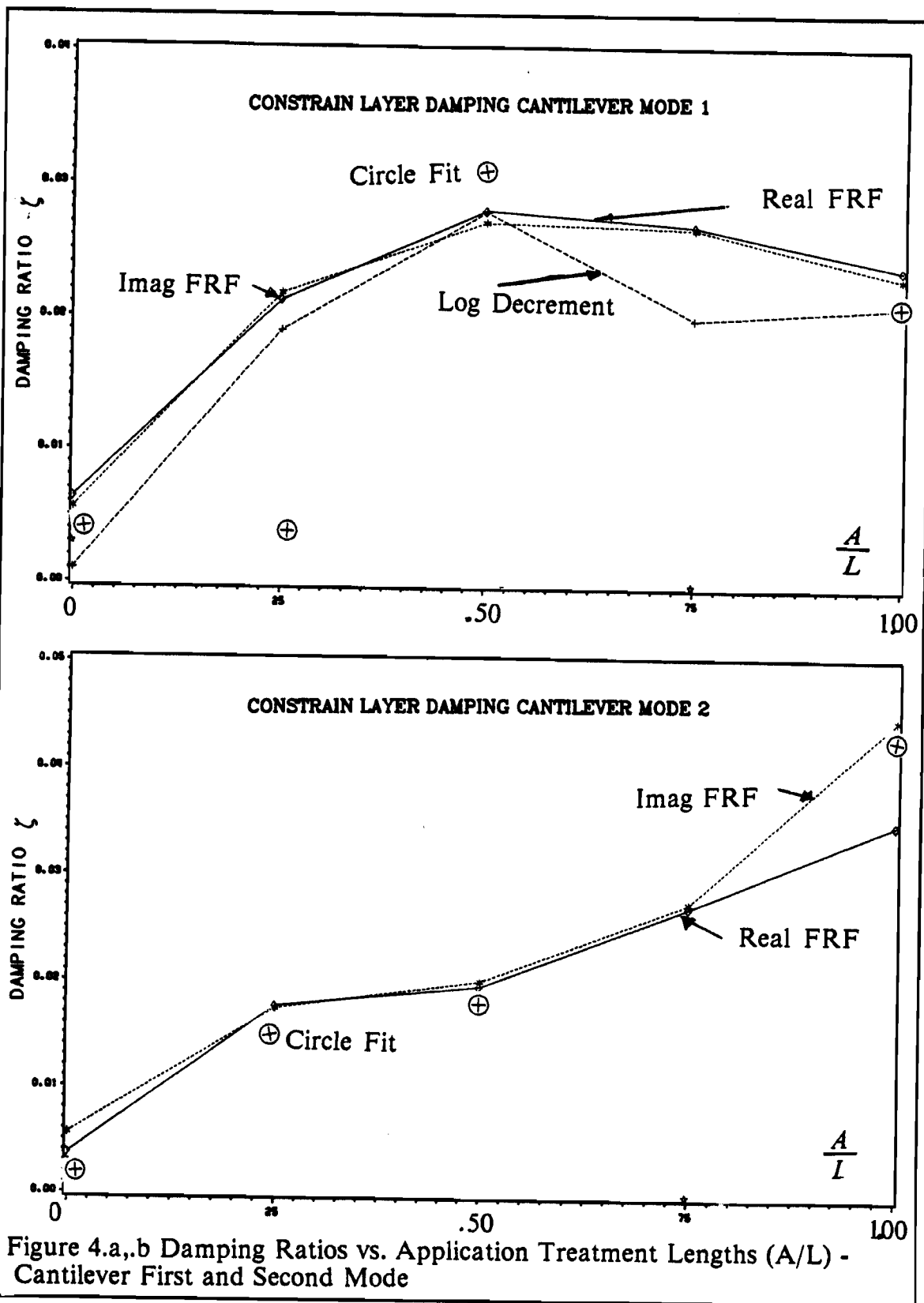
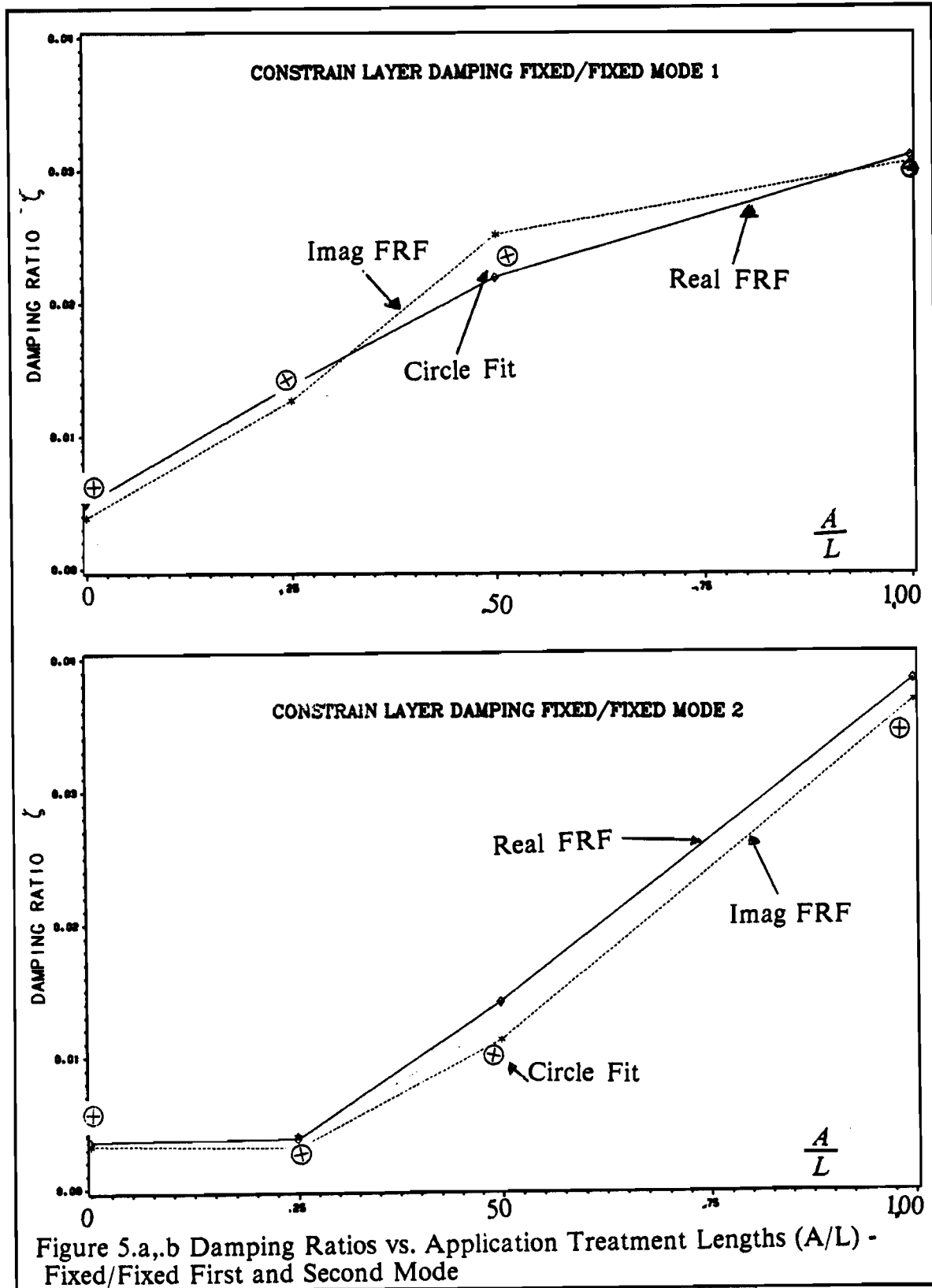
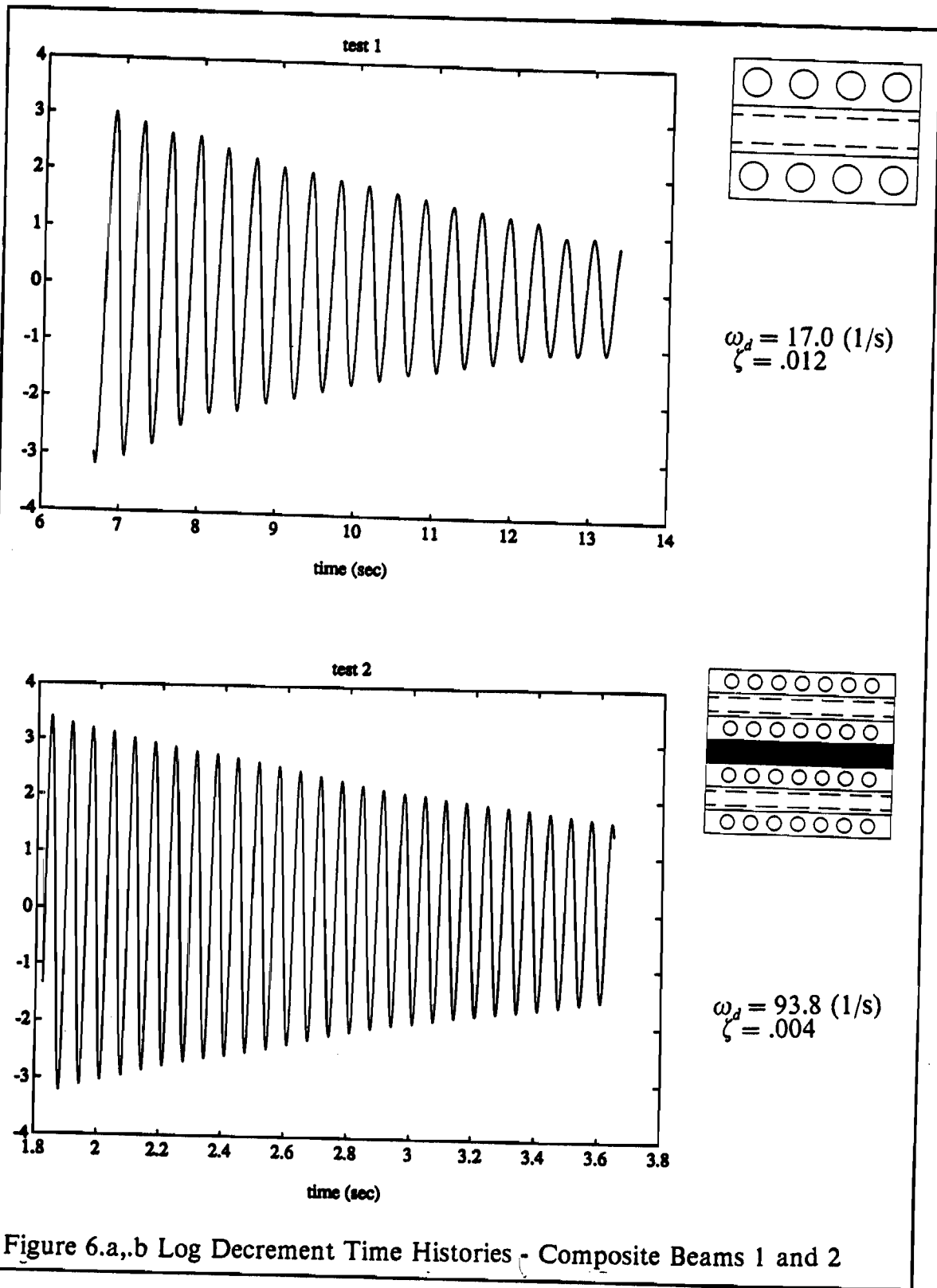
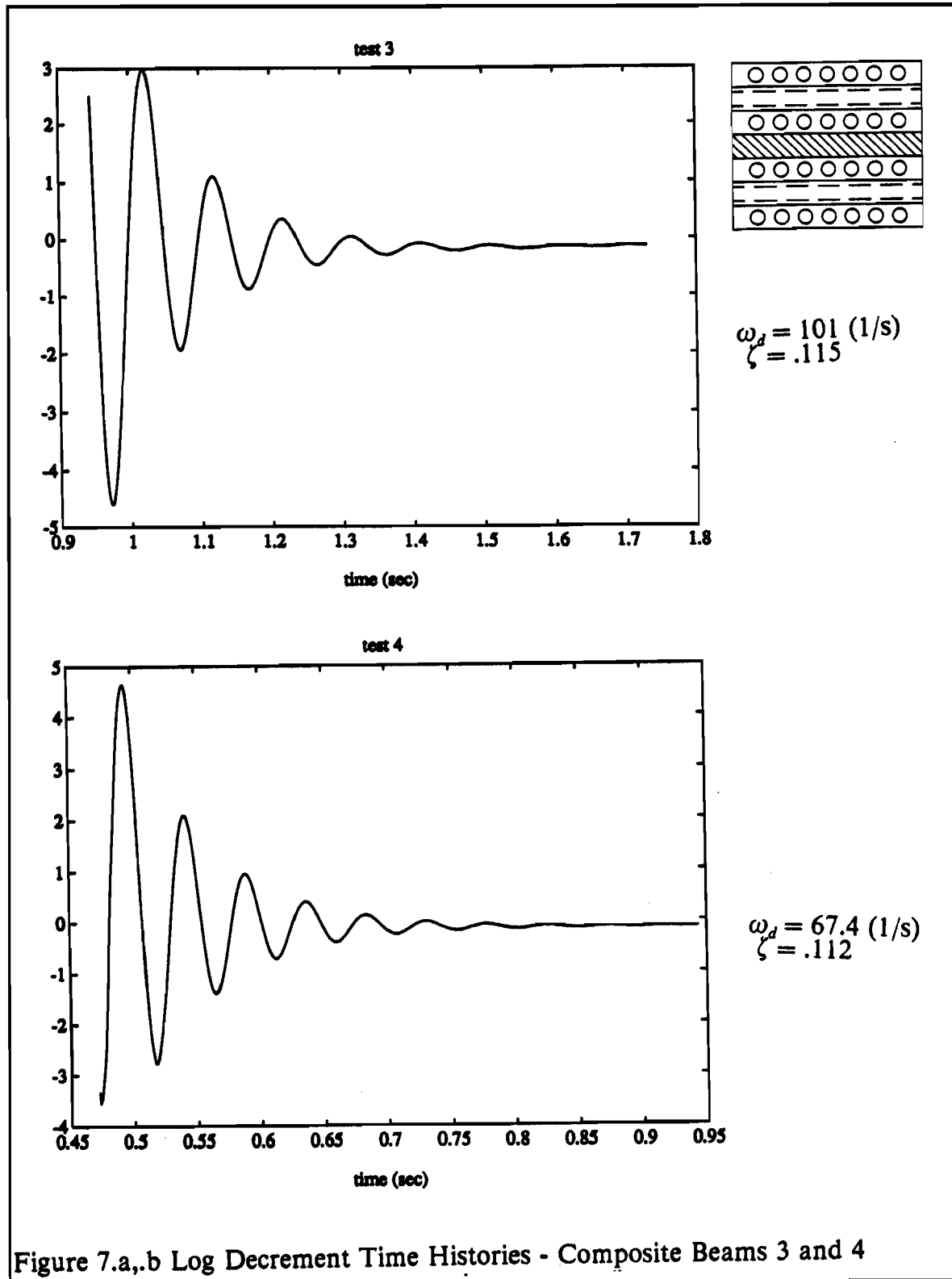


Figure 3.a,.b Magnitude and Phase of Total FRF -  $\zeta$  from .01 to .10









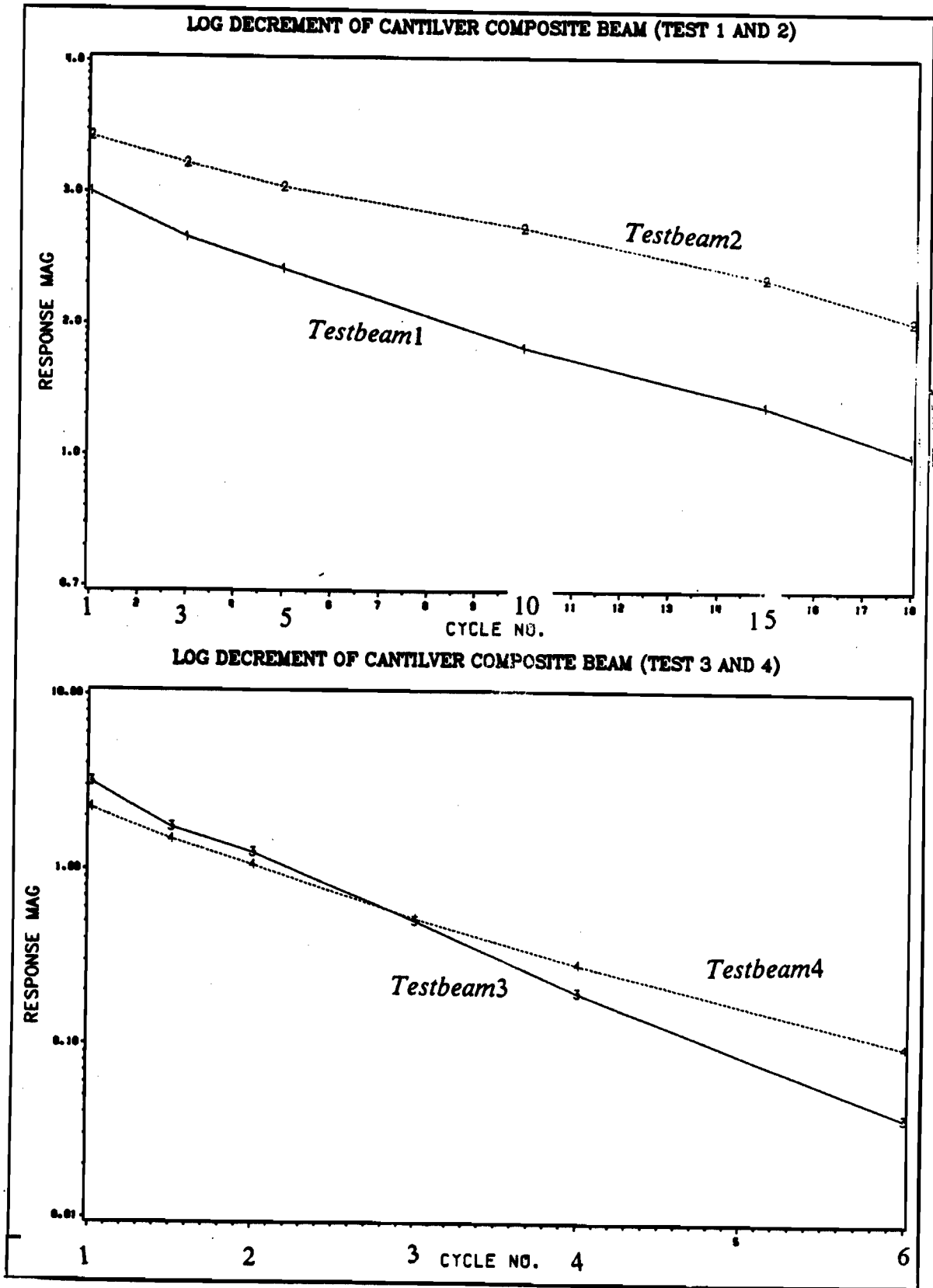


Figure 8.a, b Log Decrement Time Histories - All Composite Beams (semi-log)